Applied Energy 226 (2018) 713–729

Contents lists available at ScienceDirect

Applied Energy

journal homepage: www.elsevier.com/locate/apenergy

A Review of Transparent Insulation Material (TIM) for building energy saving and daylight comfort

Yanyi Sun*, Robin Wilson, Yupeng Wu*

Department of Architecture and Built Environment, Faculty of Engineering, The University of Nottingham, University Park, Nottingham NG7 2RD, UK

HIGHLIGHTS

- Transparent Insulation Materials offer the potential to improve building performance.
- State-of-the-art review on methods to characterise Transparent Insulation Materials.
- Review of methods used to comprehensive evaluate TIMs for building application.

ARTICLE INFO

Keywords:
Transparent Insulation Materials (TIM)
Thermal performance
Optical performance
Experimental investigation
Numerical investigation

ABSTRACT

Improving the energy efficiency of buildings is a key strategy in responding to climate change and resource challenges associated with the use of fossil fuel derived energy. The characteristics of the building envelope play a decisive role in determining building operation energy. Transparent Insulation Materials (TIMs) add to the strategies that may be used to sustain these improvements: they can reduce heat loss by providing high thermal resistance while effectively transmitting solar energy and contributing to the luminous environment. In this review, key types of TIMs and their characterisation in terms of both thermal and optical behaviours are introduced as well as the benefits that may be realised through their application to buildings. Relatively few studies exist regarding the performance of window systems incorporating TIMs. To provide a clear picture of how to accurately predict the performance of TIM integrated window systems, this paper also explores the literature around window systems incorporating complex interstitial structures, as these share many of the same characteristics as TIMs. The experimental and numerical methods used to evaluate the thermal and optical characteristics of complex window systems are summarised and this body of research provides potential methods for tackling similar questions posed in relation to the performance of window systems with TIMs. Finally, this review introduces a method that permits the prediction of the combined thermal and daylight behaviour of spaces served by TIM integrated window systems. The results from using this methodology show that using TIMs over a conventional window system offers a range of benefits to the occupants of buildings. Thus, this review offers a workflow that may be used to assess and analyse the benefit of applying TIMs for building energy saving and daylight comfort in buildings subjected to varying climate conditions.

1. Introduction

Buildings currently account for 30–40% of the world's total primary energy demand [1,2]. Energy efficiency requirements are continuously improved through stricter stipulations in building regulations [3–5]. In the UK's Building Regulations Part L: Conservation of fuel and power [6–9], the current edition (2013 edition with 2016 amendments) introduced a reduction in target emission rate of 25% as compared with the previous edition (2006) [10]. This was accompanied by a decrease of target U-values for building components, increase in the envelope airtightness and increased requirements to control unwanted solar gains, to avoid excessive summer temperatures [11].

In response to evolving standards of building regulation and to satisfy the growing expectations of occupant comfort, the performance of building envelopes has undergone sustained improvement over a period of several decades [12–14]. Increasing the thermal resistance of the building envelope is one of the most effective approaches to reduce heat loss (or gain) and in so doing reduce the required energy consumption for maintaining a desired level of indoor thermal comfort [15]. Applying conventional insulation products (e.g. expanded polystyrene (EPS), extruded polystyrene (XPS) and mineral fibre products) to the building envelope is a common and mature practice to increase thermal

* Corresponding authors.
E-mail addresses: Yanyi.Sun@nottingham.ac.uk (Y. Sun), Yupeng.Wu@nottingham.ac.uk (Y. Wu).

https://doi.org/10.1016/j.apenergy.2018.05.094
Received 27 December 2017; Received in revised form 28 April 2018; Accepted 23 May 2018
Available online 14 June 2018

resistance [1]. Novel insulation technologies such as Vacuum Insulation Panels [3] and aerogel [16] can provide the required thermal resistance using layers that are much thinner than conventional insulation materials and hence reduce the thickness of the building structure. Amongst the various components that form building envelopes, window systems, which can be responsible for as much as 60% of the total energy consumption of a building [17], are exceptionally important elements. This is because windows systems contribute to both heat gain and heat loss through the building envelope and also determine daylight distribution and daylight availability [18]. A strategy that involves the integration of Transparent Insulation Materials within a double-glazing unit offers the potential to deliver combined improvements in thermal, solar and daylight performance [18–21]. However, relatively few studies exist regarding TIMs' building application in this manner as most of the previous research into TIM concentrates on its application in solar collectors and in solar walls. Additionally, detailed analysis of the balance between the thermal resistance and solar transmittance of TIMs and the impact these have on building performance has been less rigorously explored and only a few studies have been conducted to analyse their energy efficiency when subjected to varying climate conditions [21]. There is also a role for a systematic review that summarises the key experimental and numerical methods for evaluating the thermal and optical characteristics of window systems containing TIM.

This paper presents the current research status into TIMs. The studies reviewed have been traced back to the 1960s when the use of Transparent Insulation Material (i.e. honeycomb structures) in a flat-plate solar collector to suppress convective heat transfer was first reported [22–24]. From the 1970s to the mid-2000s, a number of studies, which experimentally and/or theoretically investigated TIM's ability to suppress natural convection were undertaken and are summarized in this review [25–49]. In the past decade, aerogel, which is a typical homogenous TIM structure, has attracted lots of attention and research interest in the field of building energy efficiency [3,16,50–56]. However, numerical simulation techniques and sophisticated measurement techniques, which have witnessed fast growth during the past decade, have seen less application in the research of TIM. Thus, this review also introduces up-to-date methods that can be used to characterise the thermal and optical performance of many TIMs, especially when applied for use in windows. With a focus on how to quantify the benefits of applying window integrated TIM to buildings, this review describes the use of dynamic daylight and energy simulation methods to predict building performance and concludes the need for more accurate daylight and energy prediction methods. The review ends by describing recent work that couples thermal and daylighting analysis to allow comprehensive evaluation of buildings employing glazing integrated TIM systems. The method may be seen as offering a first step in developing design strategies that seek to balance thermal and luminous environment of spaces served by glazing integrated TIM systems [15].

2. Transparent Insulation Materials

Transparent Insulation Materials, which seek to offer the simultaneous resistance to heat flow and facilitate the transmission of light, are almost always assembled with at least one transparent cover (e.g. glazing pane) and typically occupy the air cavity between the panes of a double pane glazing unit [57]. TIMs are generally classified under four categories according to the structure of the TIM layer and its relation with the glazing cover, as shown in Fig. 1. The categories are: (a) glazing-perpendicular structure, (b) glazing-parallel structure, (c) mixed structure and (d) homogeneous structure. There are three typical types of glazing-perpendicular structure: (1) capillary, (2) honeycomb, and (3) parallel slat array [57]. Glazing-perpendicular TIMs (Fig. 1(a1)–(a3)) divide the air cavity into small cells that run across the cavity, perpendicular to the glazing surfaces. The cell walls provide additional viscous resistance to the onset of free convection and interfere with the thermal radiation transferred from one pane of the double glazed unit to the other. Both of these effects increase the thermal resistance of the glazing system [58]. Glazing-parallel structures (Fig. 1(b)) consist of a number of glass or plastic layers arranged parallel to the glazing panes. Increasing the number of layers reduces heat loss, but results in a reduction in solar and visible transmittance due to the increased reflectance and absorbance provided by the additional layers [57]. Mixed TIMs (Fig. 1(c)) are combinations of glazing-perpendicular and glazing-parallel structures. This structure can achieve more effective convection suppression than the glazing-perpendicular or glazing-parallel structures, but see reduced daylight and solar radiation transmission. Homogenous TIMs (Fig. 1(d)) are receiving increased attention, with recent research into silica aerogel offering a translucent material that can occupy the air cavity of a double glazed unit. The high porosity of aerogels results in a very low thermal conductivity (e.g. 0.005–0.02 W/m K) [54]. There are two types of silica-based aerogels: monolithic silica aerogel (MSA) and granular silica aerogel (GSA). MSA can be clear enough to see through but its high cost and fragility currently limits commercial uptake [59]. GSA has a low solar transmittance (less than 0.5) due to bulk scattering effects and is commonly used in skylights [55,56]. Currently, the glazing-perpendicular TIMs and aerogels are receiving the greatest amount of attention in the fields of both research and industry.

2.1. Properties of TIM

- **Appearance**

The appearance of a TIM varies with the structural geometry and the material from which the TIM is constructed. Fig. 2 shows several typical designs of TIM with glazing-perpendicular structures and aerogels. It is possible to see through most of the honeycomb and monolithic silica aerogel TIMs, although at certain viewing angles disruption of the scene beyond can occur (see Fig. 2(a)–(c)). Other TIMs, such as capillary TIMs and granular silica aerogel, are more opaque in design and in addition only transmit a small proportion of incident solar energy and daylight (see Fig. 2(d) and (e)).

- **Density and temperature stability**

The density and temperature stability (i.e. the maximum temperature below which the material is stable) of TIMs are also determined by the material from which they are composed, along with their structural geometry. Table 1 illustrates the density, cell size, and maximum resistance temperature of several common TIMs.

Typically, glazing-perpendicular TIMs with capillary and honeycomb have a density of around 20–50 kg/m^3 [60]. Silicon dioxide (SiO_2, amorphous quartz) forms the basis of most aerogels; they are made up of approximately 96% air with the remainder being an open-pored silica structure [61]. The densities of monolithic silica aerogel lie between 3 and 500 kg/m^3 [60]. Those aerogels used in TIM designed also for effective transmission of solar energy are produced using supercritical drying and have density of between 100–150 kg/m^3 [60].

- **Optical properties of TIM**

The optical properties of TIM are determined by the base material characteristics (e.g. transmittance, reflectance and absorbance) as well as its geometric configuration (e.g. parallel slat arrays, honeycomb, capillary etc.). The optical properties of various TIMs have been investigated both numerically and experimentally. Numerical models for predicting the optical properties of glazing-perpendicular TIMs have been developed based on radiosity methods, and experimental investigations are typically performed using a spectrophotometer and integrating sphere.

Feland and Edwards [49], Hollands et al. [48], Symons [47], Plazer [44], Kaushika and Padmapriya [42], Plazer [37,38] and Arulanatham

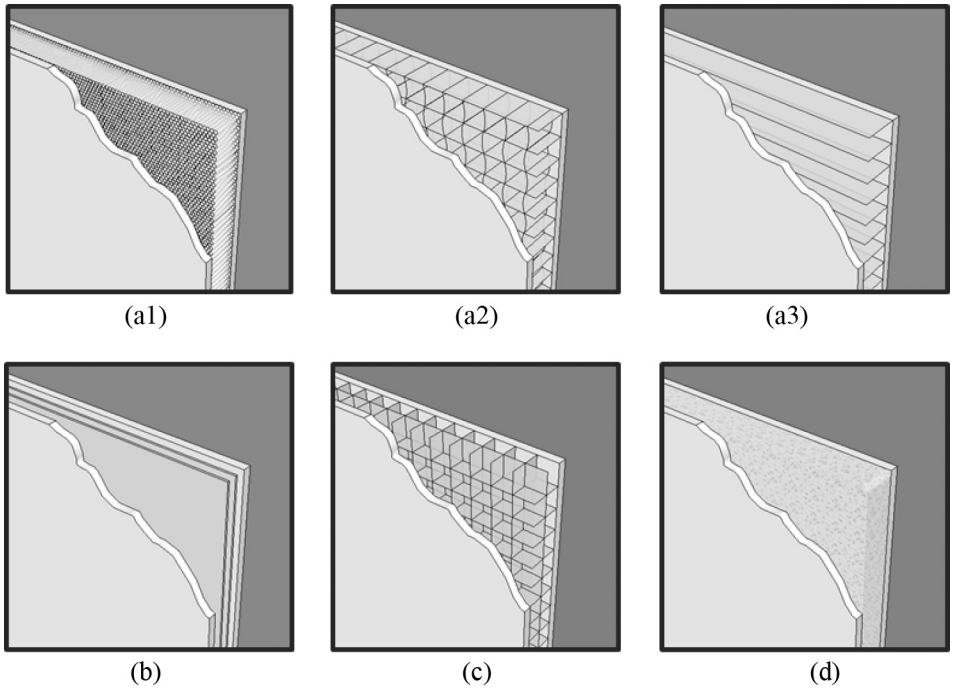

Fig. 1. Schematic diagrams of typical types of TIMs: (a) glazing-perpendicular structure: (a1) capillary structure, (a2) honeycomb structure, (a3) parallel slat array structure; (b) glazing-parallel structure; (c) mixed structure and (d) homogeneous structure.

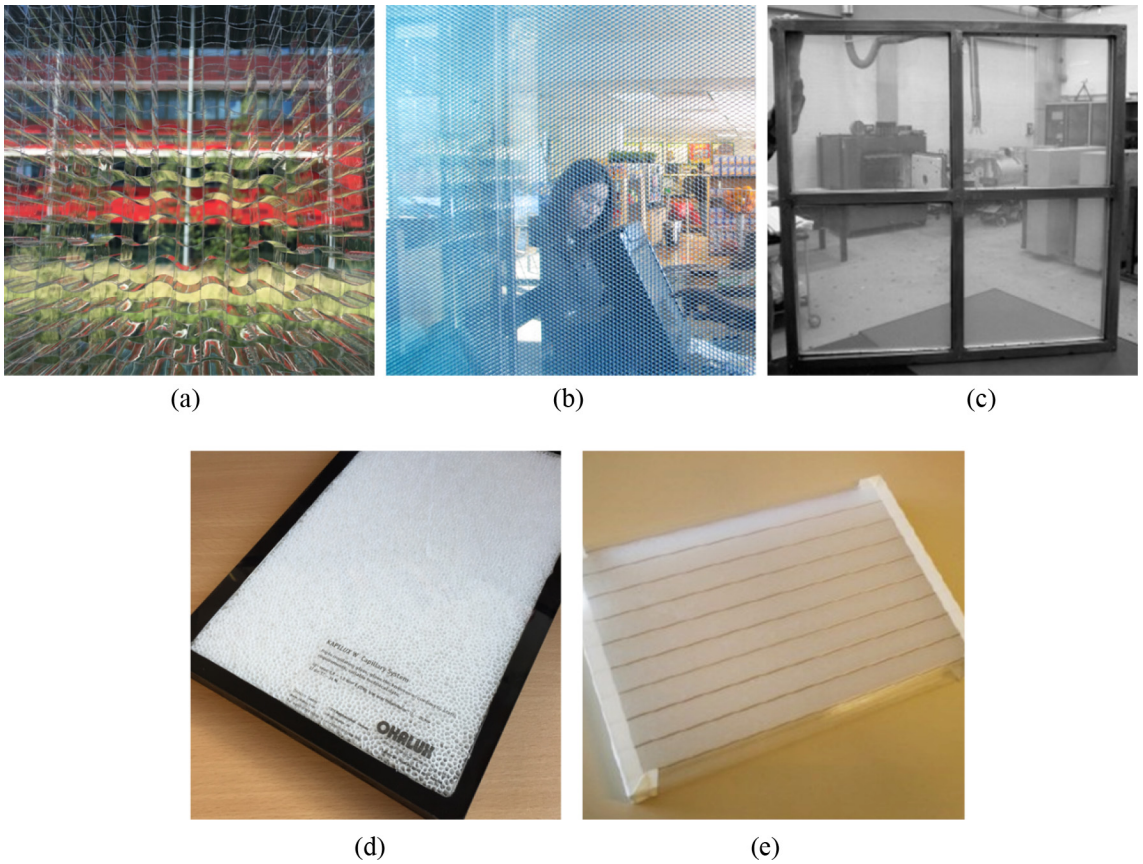

Fig. 2. Appearance of five typical TIMs: (a) honeycomb TIM from Wacotech, (b) honeycomb TIM from PANELITE, (c) monolithic aerogel from Technical University of Denmark [43], (d) capillary TIM from Okalux and (c) granular silica aerogel from Lumira.

Table 1
Physical properties of glazing-perpendicular TIMs [8]

Type	Material	Density (kg/m^3)	Cell size (mm)	Maximum temperature (°C)
Capillary	Polymethylmethacrylate	31	3	90–105
Capillary	Polycarbonate	30	3	120
Capillary	Polyethylene	18	3	160
Capillary	Polytetrafluorethylene	48	3	150
Capillary	Polyestercarbonate	30	3	175
Capillary	Polyethersulfone	36	3	215
Honeycomb	Polycarbonate	36	4.2	120
Honeycomb	polycarbonate	33	3.4	120

and Kaushika [62] analysed the optical properties of glazing-perpendicular TIMs using numerical simulation. Kaushika and Sumathy [29] summarised the research carried out by Hollands et al. [48], Kaushika and Padmapriya [42] and Arulanatham and Kaushika [62], stating that the total beam radiation transmittance at incidence angle θ, τ(θ), for TIMs based on honeycomb or parallel slats can be expressed as:

$$\tau(\theta) = \frac{\tau_C(\theta) + \tau_E(\theta)\cdot E}{1+E} \quad (1)$$

where E is the fraction of the cross-section area occupied by cell wall material. The transmittance of the wall material, $\tau_E(\theta)$, and the transmittance of the cells, $\tau_c(\theta)$, is calculated by considering the reflection, absorption and the transmission occurring at the cell surfaces. Wong [57] summarised numerical investigations conducted by Symons [47], Plazer [44] and Plazer [37,38] and concluded that, derived from the summation of all individual rays transmitted or reflected at the cell walls, τ(θ) can be expressed in a simplified form as:

$$\tau(\theta) = [\tau(\varphi) + \rho(\varphi)]^n = [1-\alpha(\varphi)]^n \quad (2)$$

where φ is the azimuth angle; ρ and α are the reflectance and absorbance at the cell wall, respectively, and n is the average number of cell wall interactions for the incoming light beam. It is possible to express n using $n = A\cdot\tan\theta$ for square honeycomb cells, where A represents the width of the square. For circular honeycomb cells, $n = 2A\cdot\tan\theta$ may be used where A represents the cell diameter.

In order to validate the theoretical predictions of τ(θ), Symons [47], Plazer [44], and Plazer [37,38] also conducted experimental studies using a spectrometer and an integrating sphere. A detailed exploration of this experimental method can be found in [15]. Wong et al. [57] concluded that the experimental results support the results from numerical calculation. The value of τ(θ) for honeycomb, parallel slat and V-slat TIM over incidence angle (θ) in the range of 0–60° is higher than 0.9 as shown in Fig. 3.

Buratti and Moretti [56,61,63] have also conducted a series of measurements for the light and solar transmittance of various aerogels (i.e. MSA and GSA) by employing a spectrophotometer (shown in Fig. 4(b)) along with an integrating sphere (shown in Fig. 4(c)), which is used to detect the diffused light transmitted through the TIM sample. The measured wavelength dependent transmission coefficient of MSA on its own and aerogels sandwiched within double glazed units is illustrated in Fig. 4(a) [61]. Monolithic aerogel offers comparatively high transmittance in the near-infrared range when compared with float glass. The results also show that there is a difference between the measured total transmittance determined using an integrating sphere and the measured direct transmittance determined without the use of an integrating sphere, thereby confirming the diffuse nature of aerogel.

- **Thermal properties of TIM**

The thermal behaviour of glazing-perpendicular TIMs has been investigated both numerically using finite difference methods and experimentally using hot-plate and hot-box experimental methods.

Numerical studies were primarily used to provide a detailed understanding of the convective, conductive and radiative heat transfer within TIMs [25,32–34]. Arulanantham et al. [34] used a finite difference method to explore the convective stability of horizontal and inclined air cavities enclosed by square honeycomb and concluded that convection suppression was affected by aspect ratio (A = L/d, where L is the thickness of the honeycomb and d is the width of the square), thickness of cell wall material (δ) and the inclination of cells (β) as shown in Fig. 5. Kaushika et al. [33] reported that a honeycomb structure offered better thermal performance for glazing units installed in a horizontal orientation but when units are inclined to more than 30° to the horizontal, parallel slat structures showed better thermal performance. Kumar and Kaushika [25] found that honeycomb structures with aspect ratio in the range between 10 and 15 were suitable for convection suppression in air cavities of depth 5–20 cm for temperature differences between 20 and 120 °C. Arulanantham and Kaushika [32] used numerical methods to study combined conductive and radiative heat transfer through a honeycomb structure in a solar collector and stated that the heat loss coefficient was determined by the interaction between the emissivity of honeycomb cell material and the nature of the absorber plate (i.e. black end plate or selective end plate) of the collector in which the honeycomb is employed.

Experiments have also been conducted to measure the thermal conductance of TIMs [27,36,38,43]. In order to evaluate the thermal conductance of capillaries, TIMs of various thickness under different tilt angles, a hot-plate apparatus consisting of a hot (i.e. 230 °C) and a cold (i.e. 5–60 °C) copper plate, heat flux meters and temperature sensors were utilised by Goetzberger [43] and Platzer [36,38]. The thickness of

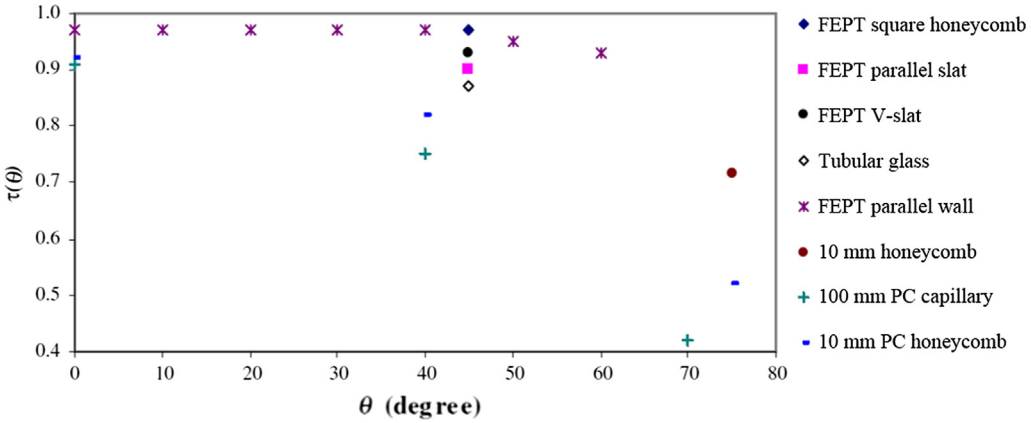

Fig. 3. Comparison of experimental results of angular dependent transmittance: τ(θ) for Fluorinated Ethylene Propylene Teflon (FEPT) square honeycomb, FEPT parallel slat, FEPT V-slat and tubular glass [47], FEPT parallel wall [44], 100 mm honeycomb [38] 100 mm PC capillary and 100 mm PC honeycomb [37,57].

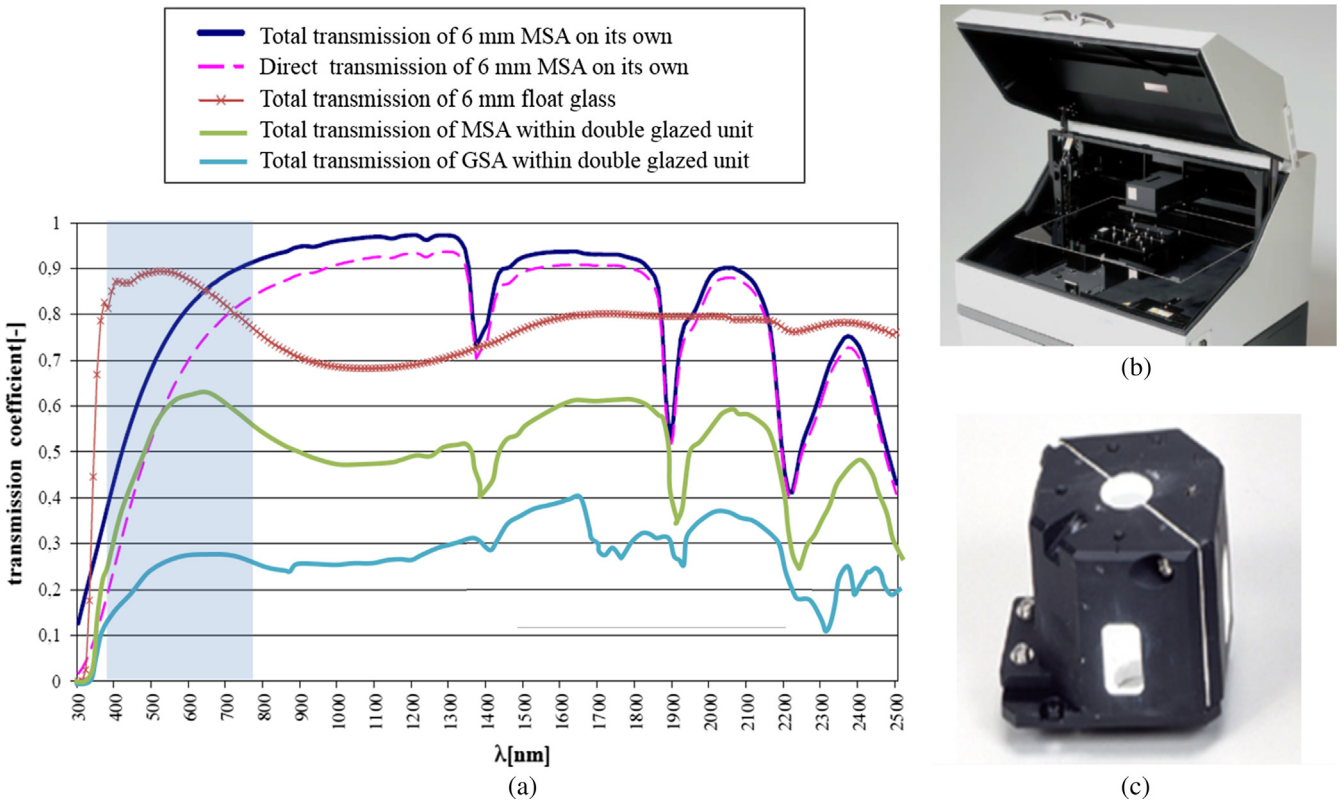

Fig. 4. Experimentally determined optical properties of TIMs: (a) measured total or direct transmission coefficient vs. wavelength of float glass, MSA on its own, MSA and GSA with double glazed units, (b) the spectrophotometer and (c) the integrating sphere, adapted from [61].

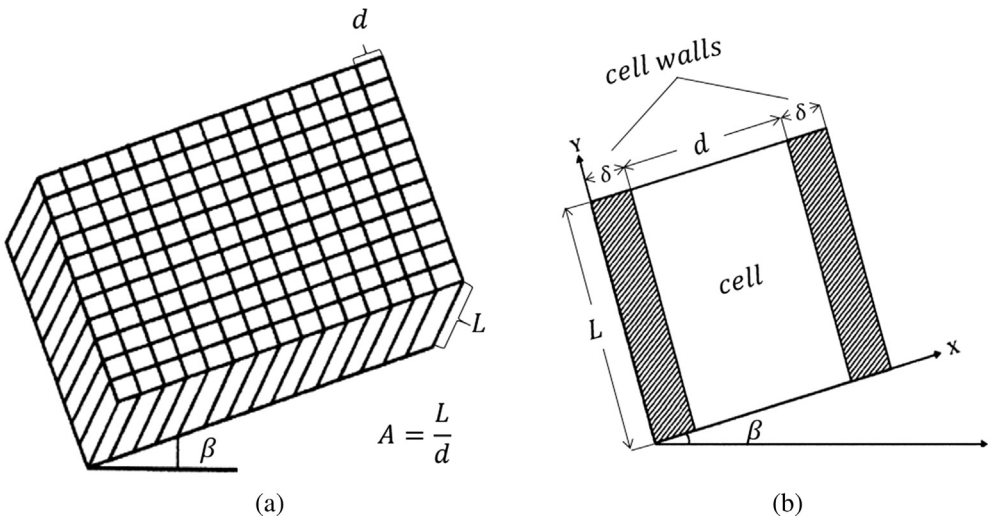

Fig. 5. Schematics of (a) square honeycomb and (b) section of a square honeycomb cell, adapted from [25].

the samples varied from 10 mm to 120 mm and the tilt angle was varied within the range of 0–180°. They also used their experimental results to validate their numerical calculation and an approximate 3.6% deviation between measurement and prediction was found when the TIM was tilted within the range of 0–55°. Suehrcke et al. [27] also used a guarded hot-plate apparatus to measure the heat transfer coefficient across TIMs with both corrugated sheet and honeycomb structure, made from cellulose acetate (CA) film with an emissivity of 0.65. They concluded that 30 mm thick CA honeycomb is more effective than 30 mm thick corrugated sheet in reducing heat loss: the heat transfer coefficient for the honeycomb was found to be 3.51 $W/m^2 K$ against 4.02 $W/m^2 K$ for the corrugated sheet. They also compared their heat transfer coefficients gained from hot-plate measurement with those of numerical simulation, and found the results agreed well with a difference of less than 3%.

Buratti and Moretti [56] used a hot-box apparatus to investigate the thermal transmittance of window systems integrating monolithic aerogel and granular aerogel and found that the windows tested with monolithic silica aerogel offered a lower U-value (0.63 $W/m^2 K$) than granular aerogel (1 $W/m^2 K$).

Recent work conducted by Sun et al. [20] used a validated Computational Fluid Dynamics (CFD) model to investigate the thermal properties of double glazing unit with integrated parallel slat TIM with different cell aspect ratios (i.e. the ratio between slat spacing and the

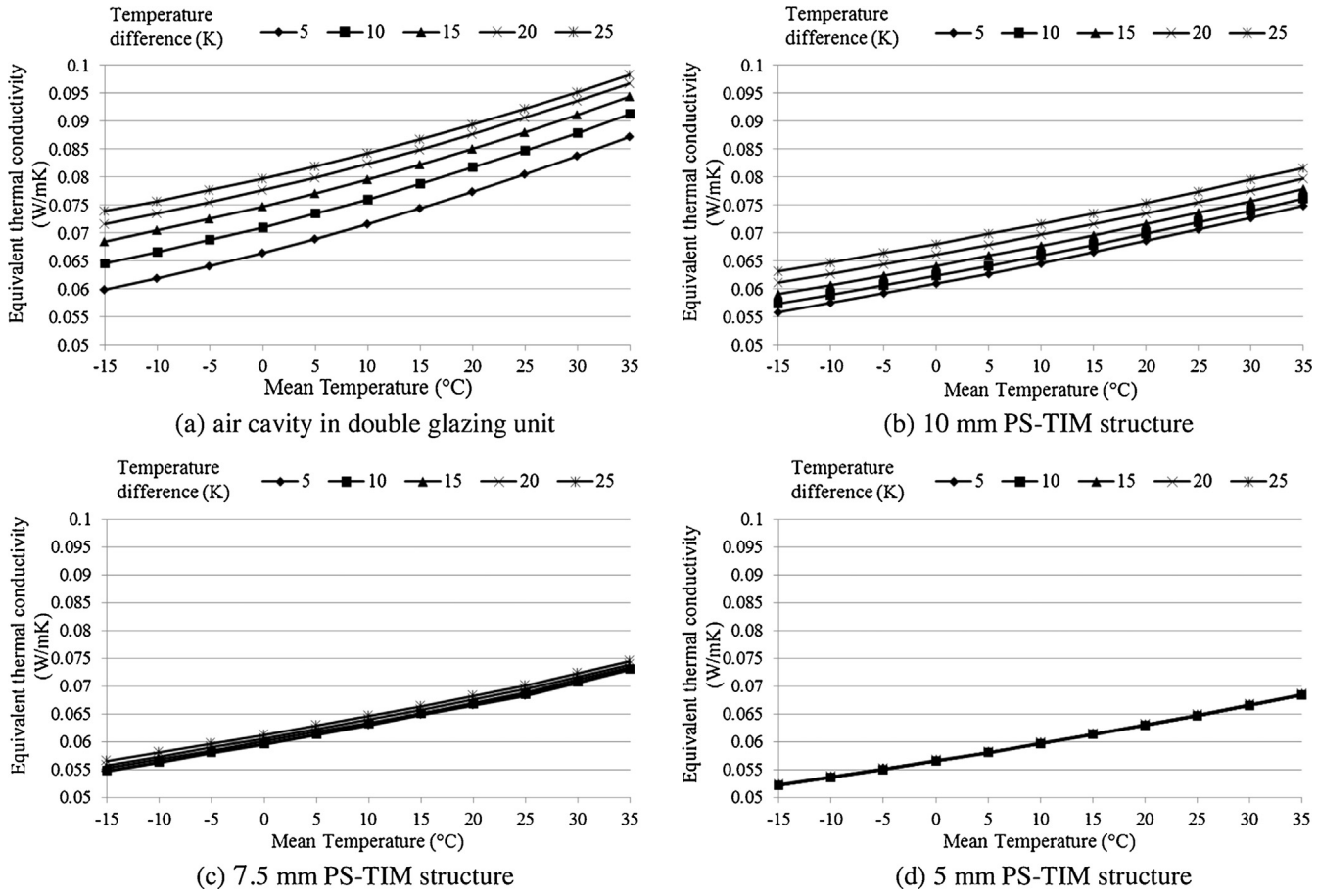

Fig. 6. The equivalent thermal conductivity of the air cavity between two glazing panes with and without PS-TIM, pre-calculated using Computational Fluid Dynamics [21].

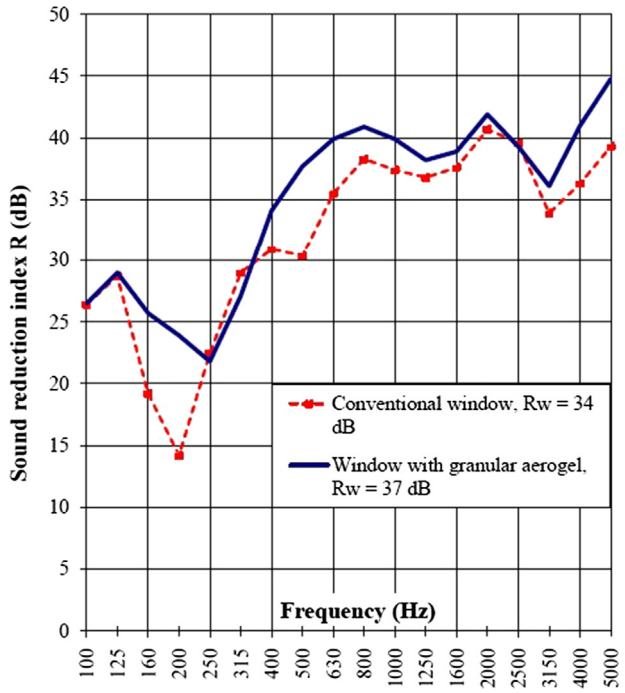

Fig. 7. Sound reduction index (R) for a conventional window and a window integrated with aerogel vs. frequency [61].

thickness of the PS-TIM layer), slat thickness and slat thermophysical properties (i.e. conductivities and emissivities). This study reveals that the presence of a PS-TIM structure can not only supress convective heat transfer but also cause a significant reduction in radiative heat transfer. The results show that an overall 35–46% reduction in thermal conductance can be achieved as compared with the same double glazing in the absence of PS-TIM and that the material properties have a more noticeable influence on small cell structures than large cell structures. In their further studies [21], the CFD simulation process was repeated for representative combinations of temperature gradient and mean temperature. Polynomial regression of the resulting conductance was used to generate an equivalent dynamic thermal conductivity of the PS-TIM layer to characterise its thermal properties. These values for both PS-TIM and ordinary double glazed units are shown in Fig. 6. From a comparison of Fig. 6(b)–(d) with (a), it is evident that the difference between each line, which represents thermal properties under varying temperature difference, is significantly diminished for windows containing 10 mm pitch PS-TIM and nearly or completely disappear when 7.5 mm and 5 mm pitch PS-TIM is present. This means that the convective heat transfer through the cavity between two glazing panes has been effectively reduced with 10 mm pitch PS-TIM and almost entirely supressed with 7.5 mm and 5 mm pitch PS-TIM. The reduction of the gradient of each line in Fig. 6(b)–(d), which represents the variation of thermal conductance with variation of mean temperature, indicate that the radiative heat transfer has been reduced through the presence of PS-TIM structure. The influence of applying PS-TIM on the window's heat gain has also been researched [21]. The simulation results show that average reductions in heat gains of approximately 38%, 42% and 46% for the 10 mm, 7.5 mm and 5 mm PS-TIMs respectively were obtained

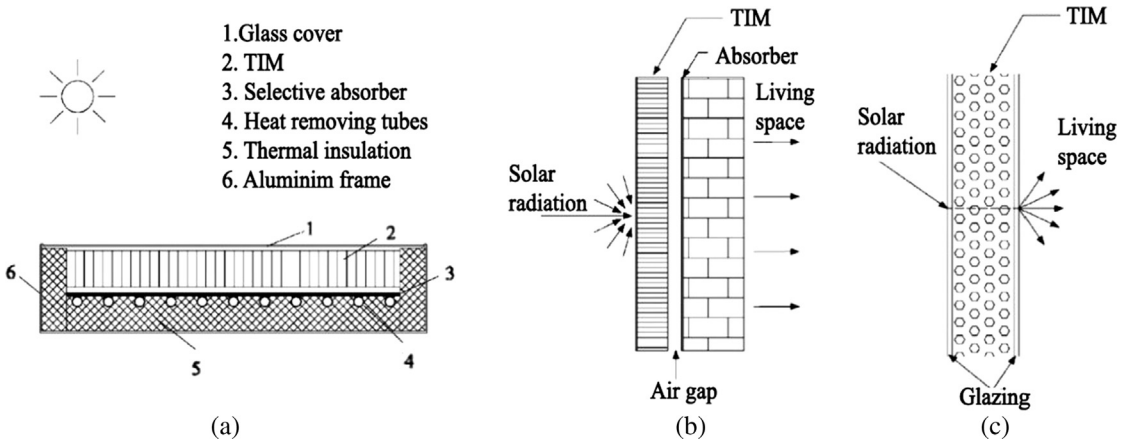

Fig. 8. Configurations of TIM in buildings: (a) in flat-plate solar collectors, (b) in solar walls and (c) in window systems or glazed façades, adapted from [29].

when compared with ordinary double-glazing.

- **Acoustic properties**

There is a small amount of research exploring the acoustic performance of aerogel based TIMs. It has been determined that window systems with granular aerogel have more efficient acoustic insulation compared with a conventional window system [61]. The measured sound reduction index, R, of double glazed windows with aerogel is higher than that of a conventional double glazed window in the range 100–2000 Hz as shown in Fig. 7. This is primarily due to the acoustic absorption provided by the aerogel, which is behaving as a porous acoustic material, and the beneficial impact that this has when present in the cavity of multi leaf structures.

2.2. Applications of TIM in buildings

There are three main ways to apply TIM in buildings: the first, and probably the earliest application, uses TIM under the front glass cover of a flat-plate solar collector; the second method, which is most often referred to as a solar wall, uses TIM in front of a thermal mass wall or a thermal mass roof; and the third method uses TIM in the air cavity of a window system or glazed façade. The configurations of these applications are presented in Fig. 8.

- **Application of TIM in flat-plate solar collectors**

Research initiated in the 1960s, primarily focused on the application of honeycomb structures in solar absorbers as a convection suppression device [22–24]. This involved theoretical and experimental research on the application of plastic/glass honeycombs to flat-plate collectors and has been expanded more recently to include studies on capillaries as well as silica aerogel [26,35,40,43,47,64]. A coefficient, named the effective transmittance-absorbance product ($\tau\alpha_e$), taking into account both transmission, τ, of the glass cover and absorption α of the absorber, was used to characterise performance. Wong [57] concluded that the value of ($\tau\alpha_e$) decreases with increase of solar incidence angle; as a result, there is a negative influence on the optical performance of the solar collectors [57]. A comparison of ($\tau\alpha_e$) at various incidence angles θ for flat-plate solar collectors is shown in Fig. 9.

This reduction in collection efficiency needs to be compensated for by reductions in heat loss if the use of TIM is to be worthwhile. For the honeycomb and capillary TIMs made of plastic or glass, Symons [47] stated that the working temperatures of the solar collectors using TIMs could be increased from 90 °C to 150 °C. Rommel and Wagner's research [35] revealed that honeycomb TIM could offer a thermal conductivity of 0.9 W/m K for the cover system at a temperature of over 80 °C. Nordgaard and Beckman's research [64] showed that the flat-plate solar collector with the integration of MSA could achieve an efficiency of more than 60% at a temperature below 80 °C and annual energy gains were increased by 41%.

As mentioned above, when TIM is integrated into a flat-plate collector, collector thermal efficiency has been significantly improved, thus the system is comparable to a vacuum tube collector [29]; however, some issues were also identified, such as the fragile and bulky nature of TIMs employing glass as the structural material, and lower stagnation temperature of TIMs made from plastic [29].

- **Application of TIM in solar walls**

Applying TIM in front of a concrete or masonry wall (Fig. 8(b)) allows solar energy to be transmitted and stored in the thermal mass while simultaneously reducing the heat loss back out through the front surface to the external environment. The combination of TIM and thermal mass was originally reported by Kaushika et al. in 1987 [45]. The system they investigated was integrated into a roof and made use of a square cell, air filled honeycomb material laid on the top of a blackened absorber and concrete slab for thermal storage. The honeycomb materials were made from 0.076 mm thick polycarbonate films or 1 mm thick acrylic sheets. In their study, $\tau(\theta)$ was calculated and found to be greater than 0.9 for the TIM made from polycarbonate film and 0.6 for the TIM made from acrylic sheet. Their results showed that with the presence of honeycomb slabs, the heat collection efficiency of the roof had been significantly improved and the heat loss during night time had been considerably reduced [45]. In their later research applying the same systems under the climatic conditions in Boulder, USA, a positive solar gain was achieved for more than 10 h during a typical winter day when the thickness of honeycomb was 15 cm [39].

The IEA Solar Heating and Cooling Programme, Task 20 [65,66] stated that the TIMs have been used as part of solar wall heating systems installed as part of building renovation measures throughout Europe. The programme also suggested that shading devices and forced ventilation should be applied to these systems in order to avoid overheating problems during summer. Braun [41] tested the performance of demonstration projects using both experimental and numerical methods to understand the space heating potential of south-facing transparently insulated massive walls. In these projects, the TIMs used were based on capillaries and honeycombs. The results showed that this passive solar façade system offers the potential to save 200 kWh per year for every square metre of collector wall. The difference between the measured and calculated temperatures of the absorber and points inside the wall was found to be less than 5 °C. Athienitis and Ramadan [30] used an explicit finite difference model to simulate the thermal performance expected when applying 48 mm of plastic transparent

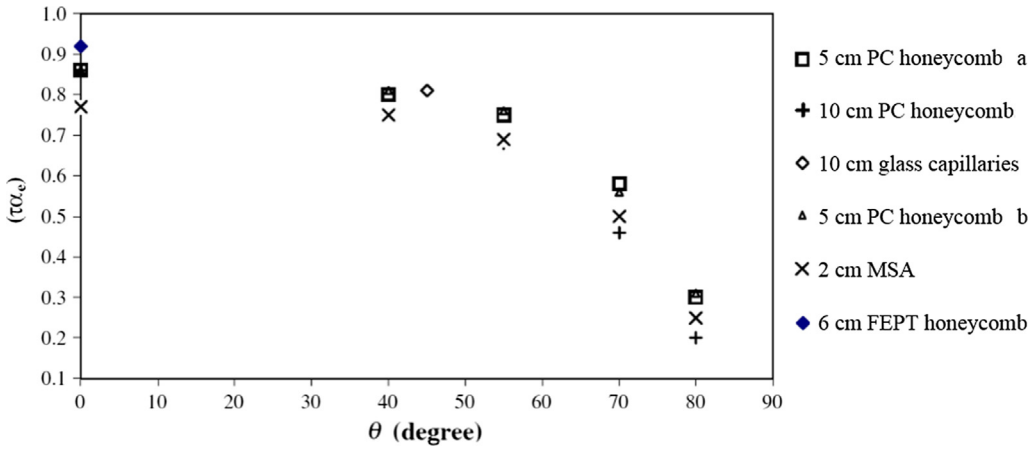

Fig. 9. Comparison of ($\tau\alpha_e$) at various incidence angles (θ) for flat-plate solar collectors with 5 cm PC honeycomb 'a', 10 cm PC honeycomb, 10 cm glass capillaries [35], 5 cm PC honeycomb 'b' [40], 2 cm MSA [64] and 6 cm FEPT honeycomb [46,57].

honeycomb (square cell) on a south-facing concrete wall, combined with a shading device and forced ventilation. They found that the application of this system to a building with a high resistance envelope reduced the heating demand to zero on a clear day with outside ambient temperatures of −20 °C – conditions representative of winter in Canada. The results also showed that the air circulation enhanced the heat transfer and succeeded in maintaining room temperature at an acceptable value. Wallner et al. [67] developed a TIM based on a novel polymer film that can be easily installed on a building façade. Their practical experience of applying 30 m^2 of this system to the south facing wall of well insulated test house showed a solar energy efficiency of 44%, U-value of 0.76 W/m^2 K and heat fluxes of up to 50 W/m^2 on cold sunny days can be achieved.

Solar walls using Phase Change Material (PCM) in place of traditional concrete or masonry walls have been investigated by a number of researchers. Manz et al. [68] conducted both experimental and simulation studies on a prototype TIM-PCM wall in Zurich, in Switzerland. A layer of 12 mm PMMA capillaries was applied in a double-glazed window in front of PCM in a glass container. The spectral direct-hemispherical transmittances of two PCM samples were measured. The predicted performance of the TIM-PCM system in the month with lowest irradiation (December) showed that energy losses through the façade occurred for only 1% of the month. Heim [28] also conducted simulation studies using ESP-r software to investigate a TIM-PCM wall on a south façade concluding that this design could reduce the temperature fluctuation of inside surfaces. Wong et al. [43] investigated the application of 22 mm PMMA capillary TIM in solar walls on a south facing façade of high-rise and low-rise office buildings. Their simulation results for a full calendar year showed that the room temperature swing during the daytime was reduced. The TIM solar wall was shown to offer good potential to reduce heating energy load during winter; but it was observed that overheating problems might exist in summer.

- **Application of TIM for window systems or glazed façades**

When used in windows, TIMs have the potential to significantly reduce heat loss while also maintaining light and solar transmittance; moreover, the use of TIM can result in a more homogeneous internal daylight distribution thereby improving visual comfort level. Thus, applying TIM in window or glazed façade systems can result in a reduction in both lighting and space heating energy consumption for the spaces they serve. However, TIM window and glazed façade systems have not been as extensively researched as the use of TIMs in solar collector and solar wall applications.

Twidell et al. [69] undertook a three year monitoring project in order to investigate performance of two blocks of five-storey university residential buildings in Glasgow, UK following the application of TIM glazing on the south façade. The system consisted of a 100 mm thick layer of honeycomb with 3 mm square cells, encapsulated by an external glass layer. The results showed that during the wintertime there was 40% less energy consumed as compared with best practice building energy performance prevailing at the time. The financial savings of 30% in heating energy were obtained and the systems offered a 20 year payback period.

Lien et al. [31] researched the performance of glazing with capillary TIM in terms of daylight distribution, appearance as a facade material, visual contact for observers inside buildings to the external environment, and energy consumption when applying capillary TIM to terraced houses. In their research, the daylight distribution performance was tested through use of scale models and artificial light sources. The profiles of daylight distribution at different incidence angles (representing four different times of day for an equinox at a latitude of 63°N) for a window with and without TIM are presented in Fig. 10. Compared with clear glass (Fig. 10(a)–(d)), the light transmitted through the capillary TIM (Fig. 10(e)–(h)) is more evenly distributed through the room showing an absence of any of the obvious sun patches observed in the room with conventional glazing. The comparison also shows that incoming light from lower sunlight altitude (Fig. 10(e)) spreads the light over larger areas, and also deeper into the room. The researchers also conducted a computer simulation using SUNCODE, applying a capillary-based TIM of various thicknesses (35 mm, 100 mm and 200 mm) to the south façades of dwelling houses. The results revealed that replacing part of a traditional south wall with a TIM integrated façade (i.e. 5 m^2 TIM glazing plus 0, 15 or 25 m^2 TIM solar wall) saves up to 8% of heating and lighting energy. Overheating risks were also predicted but it was observed that these could be mitigated if the ventilation rate was increased and that this may be achieved by natural means through the integration of air vents into the TIM facade. Applying the TIM was found to result in only 0.2–1.8% increases in cooling demand while heating demand reduced by 3.7–6.1%. Lien et al. [31] also described the visual features of their capillary TIM, and highlighted that the visual contact is both limited and disrupted, the extent being related to the thickness of the TIM, as well as the distance and angle from the viewpoint. Increasing the distance from the viewpoint to the TIM provides a larger range of vision, whereas increasing the thickness of capillary TIM decreases the range of vision. Larger diameter capillaries also result in a larger transparent area. It was found that if the capillaries have a diameter of less than 1 mm, nothing can be seen through the material, which instead appears to be white in colour.

Bahaj et al. [70] investigated the energy performance of a high-rise commercial building in Dubai where an aerogel glazed façade was used to replace a conventional glazed façade. It was found that the aerogel

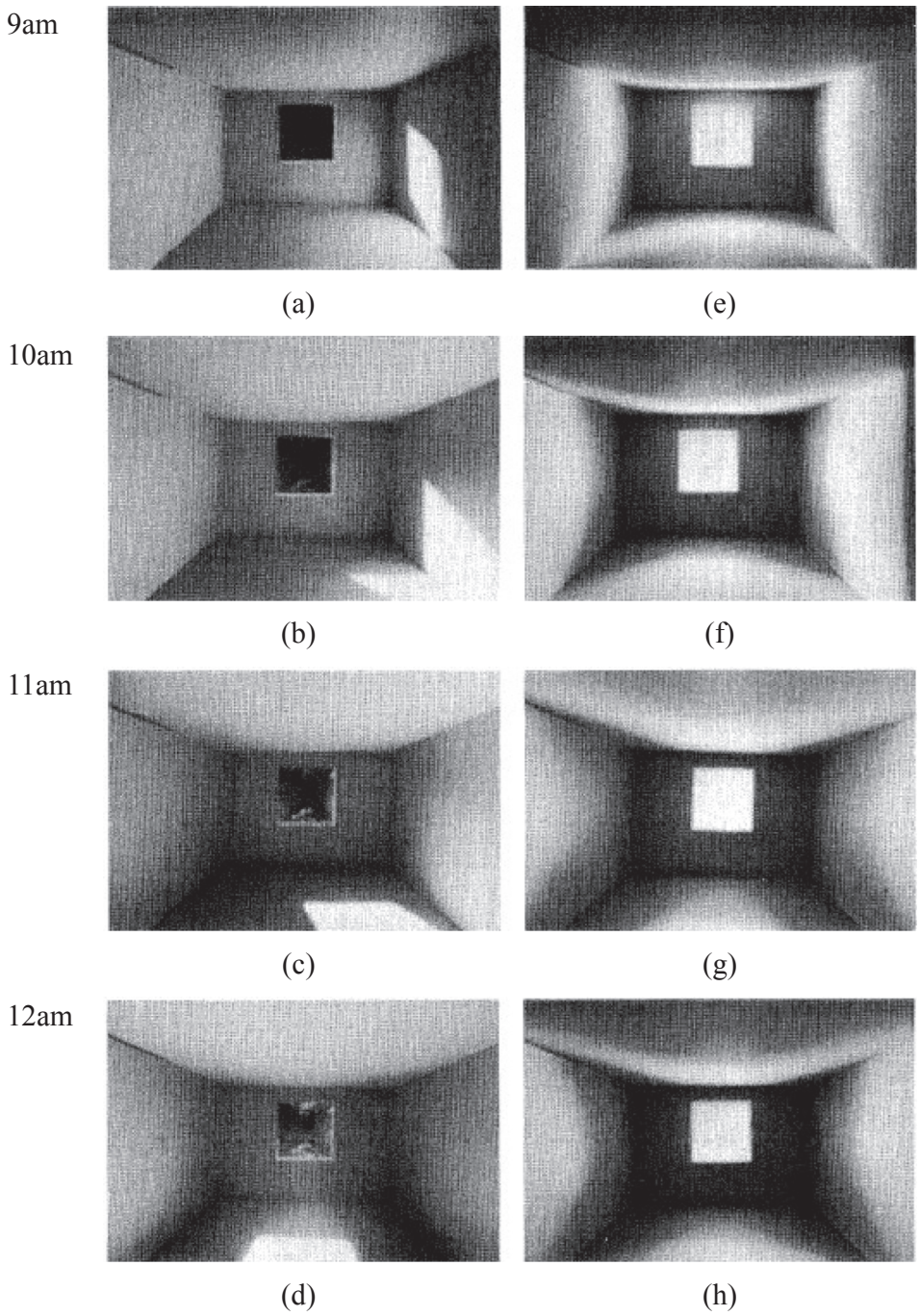

Fig. 10. (a)–(d) Sunlight distribution through clear glass for an equinox in Trondheim, at 63°N; (e)–(h) sunlight distribution through 35 mm capillary TIM for an equinox in Trondheim, at 63°N [31]

glazed façade could reduce air conditioning demands by approximately 17%. When the aerogel glazing was combined with a reflecting component (holographic optical elements) incorporated in the glass laminate, air conditioning savings of approximately 26% were achieved.

Sun et al. [18,21] investigated the application of PS-TIM to a window in a small office and tested its performance under five different climate scenarios (i.e. Stockholm, London, Beijing, Hong Kong and Singapore). The heating, cooling and lighting demands in EnergyPlus and the daylighting performance of the glazing systems in RADIANCE were predicted. The results indicate that the inclusion of PS-TIM systems improved the luminous environment by reducing the hours of over illumination and in so doing resulted in a more uniform illumination of the working plane under all five climates. Also, as can be seen from Fig. 11, cooling is the dominant mechanism through which energy savings were made when integrating PS-TIM into building windows. The largest potential for saving energy was in Singapore, which is a representative of hot climate [21].

2.3. Summary of current research status and industrial development of TIMs

The light transmittance, solar transmittance and thermal properties of TIMs have been studied both experimentally and theoretically as discussed in Section 2.1. However, most of the fundamental studies of the thermal and optical characteristics of TIMs focus on their application in solar thermal collectors. The integration of TIMs within building

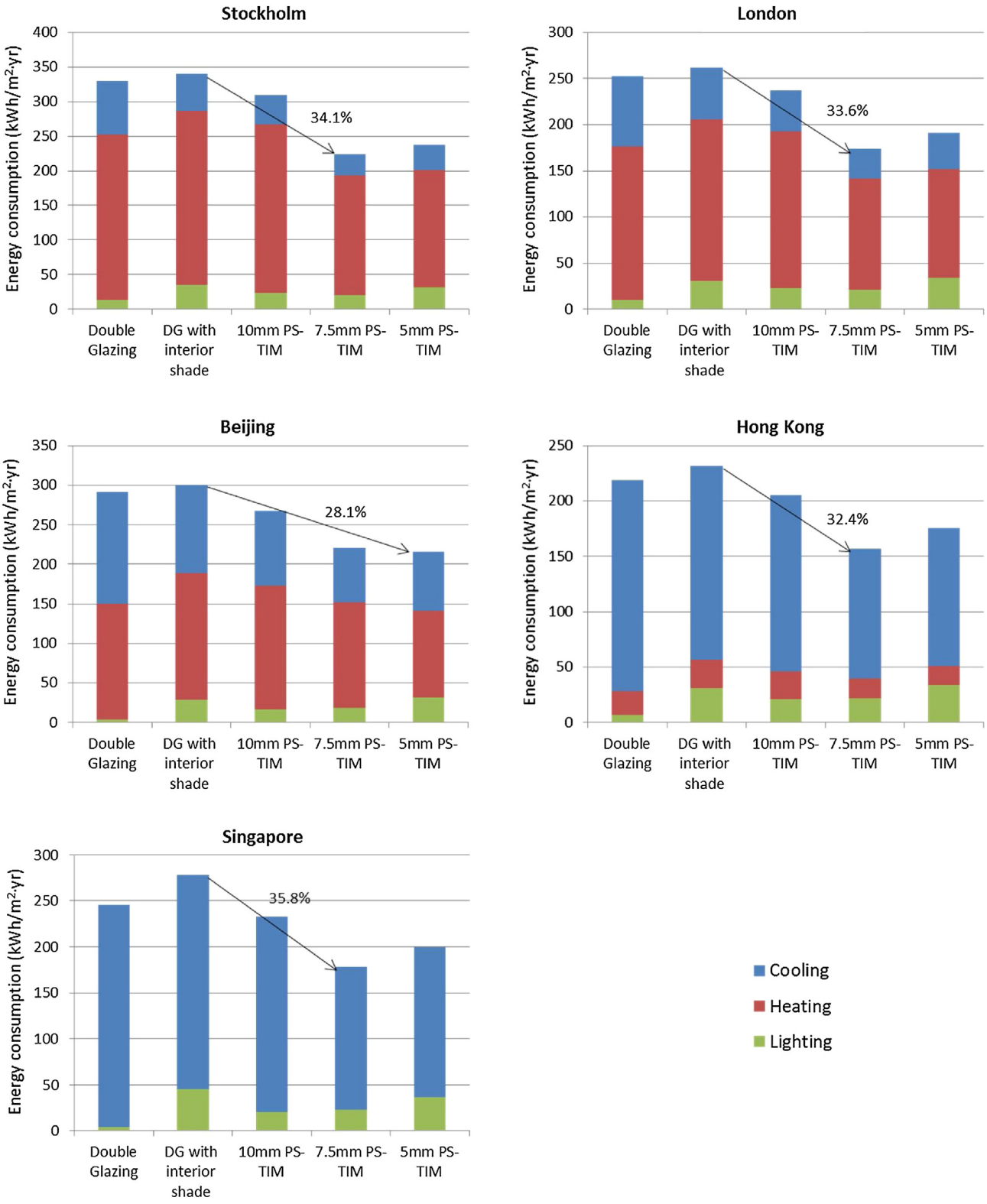

Fig. 11. Annual heating, cooling and lighting energy consumption when HVAC system is operated continuously [21].

windows or glazed façades has received much less attentions.

In order to apply TIMs in buildings, their thermal performance and efficiency, as well as the heating and cooling energy conservation potential have been monitored and simulated using computer software as discussed in Section 2.2. A particularly important issue that complicates the application of TIM to buildings is the problem of overheating during summer. Various strategies have been proposed in order to solve the issue of overheating, including mechanical shading devices, forced ventilation and the addition of spectral selective or thermotropic layers. However, a holistic analysis of the energy efficiency of TIMs subjected to varying climate conditions has not yet been conducted. In addition, the daylight performance of TIM applied in buildings has still not been thoroughly researched and discussed.

In recent years, TIMs have become a commercially interesting

product. Companies that have connections to the glass industry or related fields, for example OKALUX, Panelite, Lumira and Wacotech, have manufactured and launched a range of TIMs. The most common TIMs used in the commercial market are honeycomb, capillary and granular aerogel. However, the TIM market is still very limited. The obstacles to large-scale marketisation of TIM include restricted access to information [71], imperfections associated with the manufacturing process, and the relatively high costs involved.

It is clear that TIMs have a role to play in reducing the thermal conductance of building envelopes, and improving both solar gain and daylight performance. These three areas of behaviour influence the environment and energy performance of any space separated from the external environment by envelope components with integrated TIMs. Improving the current understanding of these individual performance criteria beyond its current state would assist significantly in developing holistic models that permit a more realistic picture of the nature of the environment and energy demand of buildings integrating TIM.

3. Thermal and optical investigations of integrating TIM into window systems

As mentioned in Section 2.3, although the thermal and optical performance of TIMs applied to windows have seen relatively little research, the concept of using interstitial structures, such as horizontal Venetian blinds, pleated blinds, etc. within the air cavity of a double glazing unit has been widely researched. These structures share many of the same characteristics as TIMs and this body of research therefore provides potential methods for tackling similar questions posed in relation to the performance of window systems with TIMs. Previous experimental and numerical methods used to thermally and optically characterise these complex window systems are summarised and discussed in this section.

3.1. Thermal investigation

- **Experimental methods**

When presented with the need to measure the steady-state thermal properties of a building component under laboratory conditions, the hot-plate method, heat flow meter method and guarded or calibrated hot-box method are the three key approaches that may be used. In these three methods, hot-plate and flow meter methods are suited to the characterisation of homogeneous materials, such as single glazing, insulation materials etc. while the hot-box method [72–76] is more widely used to measure the overall heat transfer through large, inhomogeneous structures, such as glazing system with frames or interstitial structures [77]. The specimen is mounted between two chambers that are kept at stable hot and cold conditions. The hot chamber serves as a guard to a metering box, which is mounted over the test sample. By maintaining equal temperatures in the hot chamber and the metering box, all the heat supplied to the metering box is assumed to be transmitted through the sample. Measurement of the energy supplied to the metering box is then used to determine the thermal transmittance of the sample [78]. Chen et al. [79] conducted hot-box measurement under summer conditions for double glazed units with and without embedded semi-transparent thin-film photovoltaics. The experimental results for a double glazed unit revealed a difference of less than 5% when compared with simulation results obtained by using WINDOW and THERM software. Asdrubali and Baldinelli [80] compared three hot-box methods according to ISO 8990 [72], ASTM C1363 [73] and GOST 26602.1 [76] respectively. The results revealed that ISO 8990 and ASTM C1363 are very similar since they only measured the total heat transfer through the specimen; while GOST 26602.1 measured individual thermal characteristics of each component of the specimen, giving more information on the weaknesses and strengths of these components. Baidinelli and Bianchi [78] used the same hot-box apparatus to measure the thermal conductance of windows with wood and aluminium frames. Fang [81] studied the centre-of-glass U-value of a window with high-reflectivity Venetian blinds using a hot-box configuration. The influence of the blind's slat slope-angles on U-values was evaluated and an empirical correction factor for the window U-value was proposed. Fang et al. [82] made comparative tests of flat vacuum glazing systems between guarded hot-box measurements and finite element model simulations. The resulting flanking loss, overall heat transfer coefficients and mean surface temperatures showed good agreement.

The dynamic thermal properties of window systems measured under more realistic environmental conditions, can be determined in in-situ measurements. This method uses thermocouples and heat flux meters to measure both the temperature gradient between any two surfaces of building components, as well as the heat transfer rate through them, on the site where they are situated [83,84]. There are however, various factors that can significantly affect the accuracy of the measurements taken. These include the type and quantity of sensors used, component location, and extreme ambient conditions [83]. There are also some variables that cannot be controlled during measurements, such as external temperature, wind speed and radiant energy from the sun, which can make measurements impractical [83].

To overcome the uncertainties associated with in-situ measurement methods to simultaneously simplify guarded hot-box apparatus and streamline the process of acquiring thermal transmittance of the sample, Sun et al. [58] used an integrated method to measure the thermal characteristics of a double glazing unit with and without a Venetian blind installed in the air cavity between the two glazing panes. This measurement method followed International Standard ISO 9869-1:2014 [83], using heat flow meters to determine thermal transmittance through the sample under test. The apparatus setup was also informed by International Standard ISO 12567-1:2012 [75], using two chambers that are kept at stable hot and cold conditions to determine the temperature gradient between two surfaces of the sample. Fig. 12 shows the external view and schematic cross-section of the test chambers. The measured heat transfer rate for the double glazing unit under various temperature conditions was compared with calculated results based on standard calculation method set out in EN673 [85], and the differences were found to be less than 1%. In addition, the measured results for the glazing system without Venetian blinds were also compared with results obtained from CFD simulation, and the difference was found to be less than 4%.

- **Numerical methods**

As an alternative to experimental measurement, finite element or finite volume simulations are the most commonly used approaches to obtain the thermal properties of window systems with complex interstitial structures, especially when the air flow pattern in the cavity is of particular interest.

Computational Fluid Dynamics tools have been widely used to solve the heat transfer problem and investigate the free convection in air cavities of complex glazing systems with integrated shading devices, such as horizontal Venetian blinds, pleated blinds and different configurations of fins [86–90]. Both hot box tests [79] and laser interferometry tests [91–93] have been used to validate CFD models. Collins et al. [87] used a two-dimensional steady laminar natural convection model to investigate energy transfer through a window cavity containing louvers. They concluded that the slat tip-to-glass spacing has significant influence on the overall convective heat transfer in a window cavity with a blind. Dalal et al. [88] conducted a CFD simulation to investigate steady free convection in the cavity of a double glazed window containing a pleated cloth blind. The results show that a shorter pleat length reduces the convective heat transfer and the pleat angle is less critical in determining convective performance. De Giorgi et al. [90] used a three-dimensional FLUENT model to study the fluid

(a)

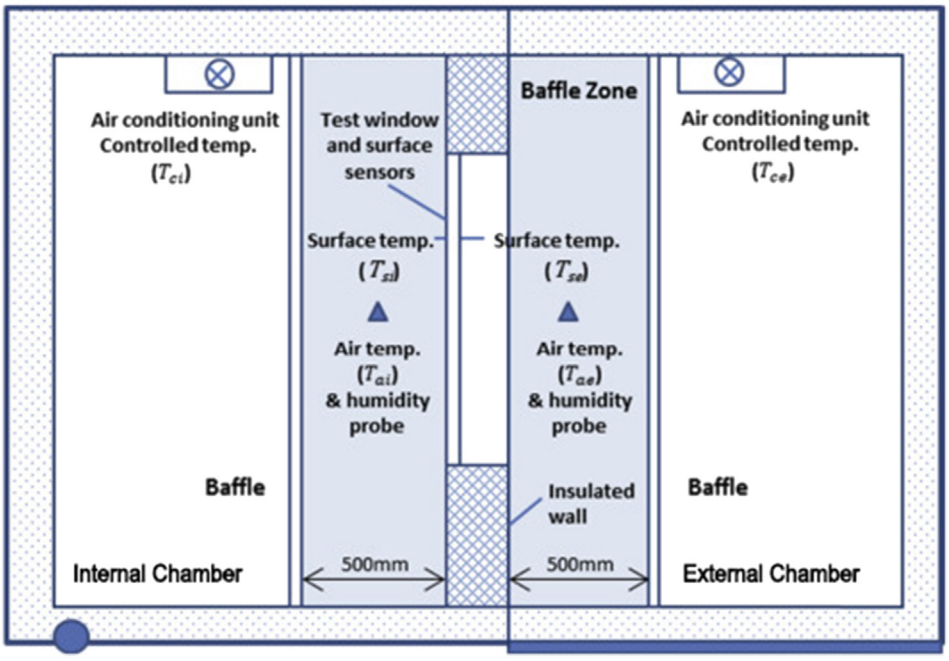

(b)

Fig. 12. (a) External view of climatic chamber and (b) schematic cross-section of the system, the test specimen and sensors [58].

dynamics inside the cavity of double glazed windows with different configurations of transparent fins (i.e. parallel fin configuration and labyrinth configuration where fins arranged to form a spiral). Their results show that presence of fins delays the onset of convection and that the parallel fin configuration appeared to be more efficient than the labyrinth configuration. In most of these studies, long-wave radiation heat transfer is neglected in the numerical modelling. Avedissian and Naylor [89] used a surface-to-surface model to include radiation in their simulation, however, they only used the model to calculate the U-value of the whole system instead of evaluating the specific effects that the internal structure has on long-radiative heat transfer. In the recent research of Sun et al. [20], instead of studying the U-value of glazing systems under a standard condition, CFD simulations of a glazing system with integrated TIMs were undertaken over a range of different temperature conditions to allow a comprehensive picture of convective and radiative heat transfer to be established, and their effects on window thermal resistance/U-value determined. A variety of cell aspect ratios, slat thicknesses and slat thermal properties (conductivity and emissivity) were examined to investigate their effects on overall thermal performance. The results from these studies were used to generate empirical correlations for the thermal resistance of double glazing units with interstitial Venetian blinds.

3.2. Optical investigation

- **Experimental methods**

The measurement of transmittance and reflectance of a building component can be obtained using a spectrophotometer in combination with an integrating sphere. A number of previous studies used this method to explore various glazing materials and window systems in terms of their respective optical performance. Jonsson et al. [94] quantified the transparency and light scattering performance in the visible range of antireflection glass coatings and an electrochromic foil. Long et al. [95] and Ye et al. [96] used a UV–visible–NIR spectrophotometer (240–2600 nm) to measure the spectral transmittance of a thermochromic film (i.e. VO_2). Goia et al. [97], Gowreesunker et al. [98], and Liu et al. [99] investigated the spectral behaviour of double glazing systems with different PCM samples. Gao et al. [52] investigated the optical properties (transmittance and reflectance between 290 and 2500 nm) of glazing units incorporating aerogel granules in the air cavity using a 150 mm integrating sphere. Berardi [53] and Buratti and Moretti [56,61,63] measured the optical behaviour of a monolithic aerogel panel on its own and sandwiched between two glazing panes with and without the use of an integrating sphere.

This method of combining a spectrophotometer with an integrating sphere is mainly suited to characterising homogenous glazing systems or materials. For a specific case of a window system that includes a complex interstitial structure, such as TIM, these standard methods can prove inappropriate as the presence of these interstitial structures can result in significant spatial deviation in the directional characteristics of transmitted and reflected flux, as well as variation in the total amount of flux transmitted/reflected. The measurements cannot capture valuable directional information that is necessary to make accurate predictions of daylight distribution in any room served by these glazing systems.

To retain information relating to the direction of entry of the light to its direction(s) of exit, recent investigators used goniophotometers to capture directional optical properties (i.e. Bidirectional Scattering Distribution Function (BSDF)) for complex window systems [100–105]. The BSDF data comprises matrices of coefficients that for light from each incident direction quantifies the proportion transmitted in each outgoing direction. A goniophotometer uses either a scanning-based method [100–105] or a video-based method [106–111] to capture reflectance and/or transmittance distribution in the outgoing hemisphere for a single incidence angle from the incoming hemisphere.

- **Numerical methods**

In order to conduct cost and time saving parametric studies, numerical methods corresponding to these experimental methods mentioned in the previous section have also been developed and validated. Radiosity methods standardised by ISO 15099 [112] are commonly used to calculate the overall transmittance or reflectance for these complex fenestration systems, such as window systems with integrated Venetian blinds [113–121], based on knowledge of the measured optical characteristics of each of the individual system components. However, this method is not suitable for models with highly specular surfaces, as it assumes that all the surfaces are Lambertian reflectors.

Virtual goniophotometers developed and validated by Andersen et al. [106,107] and Boer [122] based on commercial forward ray-tracing simulation tools (TracePro and OptiCad, respectively) can be used to obtain BSDF data for complex fenestration systems based on descriptions of their geometry and optical characteristics. Another validated program, genBSDF (implemented in RADIANCE) [123], has been used to generate BSDF data for glazing systems with integrated TIMs [18]. The generated BSDF data for these glazing systems can be used further in building daylight and energy simulation tools (e.g. RADIANCE and EnergyPlus) for determining their building performance.

4. Building performance prediction of window systems with integrated TIM

When exploring how a window with integrated TIMs performs under different climatic conditions, building performance simulation is considered to be an effective way of estimating its potential for energy saving and daylight comfort improvement. Accurate performance prediction depends on precise characterisation of the thermal and optical properties of TIM fenestration systems, in which two- or three-dimensional heat transfer and/or light transmittance might exist due to the presence of the TIM structure.

Many building simulation tools, such as EnergyPlus, ESP-r, IES, IDA ICE, TRNSYS, and TAS can be used to explore the energy and thermal performance of buildings that employ complex fenestration systems [124–135]. For daylight simulation, RAIDANCE, which is based on a backward ray-tracing algorithm (Monte Carlo ray-tracer), is regarded by many as the most accurate daylight simulation tool [108,136].

Wong et al. [137] conducted a building energy performance prediction using ESP-r software to explore the use of a TIM wall and/or TIM glazing on the south facing façades of retrofitted high-rise and low-rise office buildings in London, UK. The simulation results for a full calendar year revealed that applying TIM has the potential to reduce temperature swings during the daytime. Furthermore, the TIM also offers the potential to reduce heating energy load during winter and reduce overheating problems during summer when applied in conjunction with a mass brick wall, shading overhangs and natural ventilation.

With advances in simulation technologies, the capabilities of simulation tools to predict building energy and daylighting performance with complex fenestration systems has been significantly enhanced. The challenge related to the use of these tools for modelling windows with integrated TIM is how to establish a bridge between precise characterisation of a TIM window system and implementation of these characteristics in building simulation tools. Based on the review of potential methods mentioned in previous sections, the authors proposed a comprehensive model to investigate the thermal and optical performance of a window system with TIMs and also how they shape the daylight and energy performance of the buildings to which they are applied to [18–21]. Through this approach, the dynamic thermal conductance across the glazing system caused by variation of environmental conditions is obtained from Computational Fluid Dynamics simulation [20]. These results inform the construction of empirical equations that may be integrated into EnergyPlus to represent the thermal characteristics of the TIM in building simulation [19,21]. Meanwhile, a ray-tracing technique is used to predict the optical characteristics that were formatted into BSDF data. RADIANCE was used to generate a comprehensive picture of daylight performance when applying window systems with TIMs, quantifying performance using dynamic building daylight metrics [18]. The BSDF data are also input into the building simulation tool (i.e. EnergyPlus). Then, the developed model is used to obtain relatively accurate building heating, cooling and lighting energy estimates, when glazing systems with Parallel Slat Transparent Insulation Materials (PS-TIMs) are applied within a window [19,21]. The flow chart of each stage is shown in Fig. 13. Using this method, PS-TIMs have been applied to the glazing of a typical small office to test their performance (heating, cooling and lighting demands, and daylighting performance) under five different climate scenarios (i.e. Stockholm, London, Beijing, Hong Kong and Singapore) [21]. The simulation results show that when compared with a conventional double glazed system, the application of PS-TIMs can result in a more visually comfortable and uniformly lit environment, such as might be desired in an office space. Applying PS-TIM at higher latitudes requires smaller slat pitches to maximise useful daylight. In the specific case of the small office under test, windows with PS-TIM

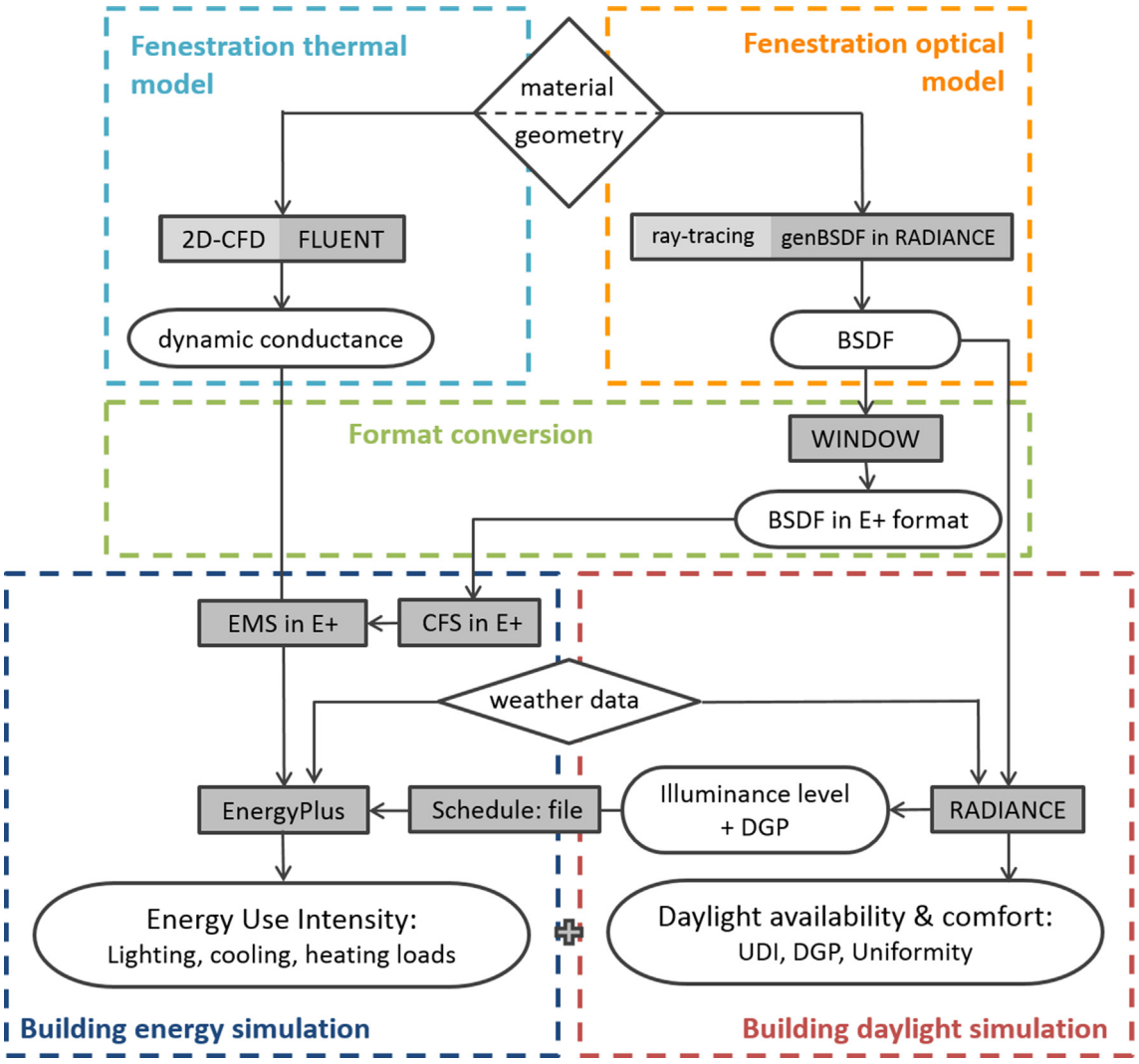

Fig. 13. Work flow of the comprehensive energy/daylight prediction method for glazing systems with PS-TIM [19,21].

can result in a reduction in energy consumption of up to 35.8%. The benefits of the PS-TIM system are more evident when the HVAC system was under continuous operation as a significant proportion of energy was saved at night due to the increased thermal resistance of the PS-TIM structure, thus mitigating against night time heat loss.

5. Conclusion

This review demonstrates that TIMs have a role to play in improving the thermal resistance of building envelopes, adjusting solar gains and affecting daylight performance. Over the past decades, the thermal behaviours of TIMs have been investigated numerically and experimentally: however much of this work focused solely on their application in solar collectors. In this guise, the application of TIMs has been proven to effectively reduce heat loss and improve solar collector efficiency. However, relatively few studies exist regarding the thermal and optical performance of TIMs contained within the cavities of double glazed windows. Here, the working temperatures, additional natural convection patterns and intensity, are significantly different. There are also the parallel considerations of impact on view (into and out of the building) and opportunities to enhance daylighting strategies that account also for visual comfort.

As relatively few studies exist that seek to effectively and accurately characterise window systems with integrated TIMs and explore their impact on building performance prediction, this review also summarised the experimental and numerical studies for characterising other complex glazing systems with interstitial structures, which share many of the characteristics of TIMs. Their bodies of research provide potential methods for tackling similar questions posed in relation to the performance of window systems with TIMs. Among the research that has taken place into windows with interstitial structures, many studies have been conducted using Computational Fluid Dynamics modelling to evaluate the possibility of reducing free convection and long-wave radiation exchange between the two panes of a double glazing unit. These CFD models have been widely validated by comparing the predicted thermal properties with results obtained using experimental tests. The optical evaluations of these complex window systems are also discussed. An advanced method that uses a matrix of Bidirectional Scatter Distribution Functions (BSDFs) to characterise the optical properties of complex window systems, is regarded as more appropriate for predicting light transmission through glazing systems with TIMs.

Based on both previous sections, the need for more efficient and accurate daylight and energy prediction methods for characterising window systems with integrated TIM is concluded. The ability to import thermal characterization into tools such as EnergyPlus as well as the ability to couple this to lighting tools such as RADIANCE creates a framework where such studies may be undertaken. In doing so, this review delivers methods to assess the impact TIMs have on building performance and explores how these may be used to analyse their energy efficiency when subjected to varying climate conditions.

Researchers, designers or engineers who are keen to develop strategies using windows with integrated TIMs that balance energy efficiency and the quality of the luminous environment of spaces can use the methodology outlined in this review to qualify their benefits.

It is worth noting that although TIM has the potential to offer improved performance of daylight distribution and yield energy saving, the designer would have to consider the extent to which they interrupt view out of and into a building. Meanwhile, the consideration of whether the daylit environment created by windows with integrated TIM, such as uniformity, are either suitable or desirable has not yet been discussed. These represent limitations of this review that require further study. The long term performance of applying TIM windows in real buildings and their economic and environmental benefit also need further research.

Acknowledgements

This work was supported by the Faculty of Engineering, University of Nottingham and the China Scholarship Council through a joint PhD studentship awarded to Yanyi Sun.

References

[1] Harish VSKV, Kumar A. A review on modeling and simulation of building energy systems. Renew Sustain Energy Rev 2016;56:1272–92.
[2] Allen K, Connelly K, Rutherford P, Wu Y. Smart windows—dynamic control of building energy performance. Energy Build 2017;139:535–46.
[3] Huang Y, Niu J-l. Energy and visual performance of the silica aerogel glazing system in commercial buildings of Hong Kong. Constr Build Mater 2015;94:57–72.
[4] Connelly K, Wu Y, Chen J, Lei Y. Design and development of a reflective membrane for a novel Building Integrated Concentrating Photovoltaic (BICPV) 'Smart Window' system. Appl Energy 2016;182:331–9.
[5] Wu Y, Gan G, Gonzalez RG, Verhoef A, Vidale PL. Prediction of the thermal performance of horizontal-coupled ground-source heat exchangers. Int J Low-Carbon Technol 2011;6:261–9.
[6] Approved Document L1A: Conservation of fuel and power in new dwellings (2006 edition).
[7] Approved Document L2A: Conservation of fuel and power in new buildings other than dwellings (2006 edition).
[8] Appproved Document L1A: conservation of fuel and power in new dwellings (2013 edition with 2016 amendments).
[9] Appproved Document L2A: Conservation of fuel and power in new buildings other than dwellings (2013 edition with 2016 amendments).
[10] BRE. Guide to part L of the building regulations e conservation of fuel and power. 2010 ed. London: National Building Specification (NBS); 2010.
[11] Pan W, Garmston H. Compliance with building energy regulations for new-build dwellings. Energy 2012;48:11–22.
[12] Lei J, Yang J, Yang E-H. Energy performance of building envelopes integrated with phase change materials for cooling load reduction in tropical Singapore. Appl Energy 2016;162:207–17.
[13] Lin Y-H, Tsai K-T, Lin M-D, Yang M-D. Design optimization of office building envelope configurations for energy conservation. Appl Energy 2016;171:336–46.
[14] Connelly K, Wu Y, Ma X, Lei Y. Transmittance and reflectance studies of thermotropic material for a novel building integrated concentrating photovoltaic (BICPV) 'Smart Window' system. Energies 2017;10:1889.
[15] Yanyi Sun YW, Wilson Robin. A review of thermal and optical characterisation of complex window systems and their building performance prediction. Appl Energy 2018;222C:729–47.
[16] Jia G, Li Z, Liu P, Jing Q. Preparation and characterization of aerogel/expanded perlite composite as building thermal insulation material. J Non-Cryst Solids 2018;482:192–202.
[17] Jelle BP, Hynd A, Gustavsen A, Arasteh D, Goudey H, Hart R. Fenestration of today and tomorrow: a state-of-the-art review and future research opportunities. Sol Energy Mater Sol Cells 2012;96:1–28.
[18] Sun Y, Wu Y, Wilson R. Analysis of the daylight performance of a glazing system with Parallel Slat Transparent Insulation Material (PS-TIM). Energy Build 2017;139:616–33.
[19] Sun Y, Liang R, Wu Y, Wilson R, Rutherford P. Development of a comprehensive method to analyse glazing systems with Parallel Slat Transparent Insulation material (PS-TIM). Appl Energy 2017;205:951–63.
[20] Sun Y, Wu Y, Wilson R, Sun S. Thermal evaluation of a double glazing façade system with integrated Parallel Slat Transparent Insulation Material (PS-TIM). Build Environ 2016;105:69–81.
[21] Sun Y, Liang R, Wu Y, Wilson R, Rutherford P. Glazing systems with Parallel Slats Transparent Insulation Material (PS-TIM): evaluation of building energy and daylight performance. Energy Build 2018;159:213–27.
[22] Tabor H. Cellular insulation (honeycombs). Sol Energy 1969;12:549–52.
[23] Hollands KGT. Honeycomb devices in flat plate solar collectors. Sol Energy 1965;21.
[24] Francia G. A new collector of solar radiant energy: theory and experimental verification. In: Proceedings of the United Nations Conference on New Sources of Energy, 4. Rome; 1961.
[25] Kaushika ND, Kumar P. Convective effects in air layers bound by cellular honeycomb arrays. J Sci Ind Res 2005;64:602–12.
[26] Ghoneim AA. Performance optimization of solar collector equipped with different arrangements of square-celled honeycomb. Int J Therm Sci 2005;44:95–105.
[27] Suehrcke H, Däldehög D, Harris JA, Lowe RW. Heat transfer across corrugated sheets and honeycomb transparent insulation. Sol Energy 2004;76:351–8.
[28] Heim D. Whole year analysis of TIM-PCM solar thermal storage wall. In: Proceeding of SimBuild 2004, IBPSA. USA National Conference Boulder, CO; 2004.
[29] Kaushika ND, Sumathy K. Solar transparent insulation materials: a review. Renew Sustain Energy Rev 2003;7:317–51.
[30] Athienitis AK, Ramadan H. Numerical model of a building with transparent insulation. Sol Energy 1999;67:101–9.
[31] Lien AG, Hestnes AG, Aschehoug O. The use of transparent insulation in low energy dwellings in cold climates. Sol Energy 1997;59:27–35.
[32] Arulanantham M, Kaushika ND. Coupled radiative and conductive thermal transfers across transparent honeycomb insulation materials. Appl Therm Eng 1996;16:209–12.
[33] Kaushika ND, Padmapriya P, Arulanantham M, Sharma PK. Transparent insulation characteristics of honeycomb and slat arrays. Energy Build 1994;19:1037–41.
[34] Arulanantham M, Singh TP, Kaushika ND. Convective heat transfer across transparent honeycomb insulation materials. Energy Convers Mgmt 1994;35:111–6.
[35] Rommel M, Wagner A. Application of transparent insulation materials in improved flat-plate collectors and integrated collector storages. Sol Energy 1992;49:371–80.
[36] Platzer WJ. Total heat transport data for plastic honeycomb-type structures. Sol Energy 1992;49:351–8.
[37] Platzer WJ. Directional-hemispherical solar transmittance data for plastic type honeycomb structures. Sol Energy 1992;49.
[38] Platzer WJ. Calculation procedure for collectors with a honeycomb cover of rectangular cross section. Sol Energy 1992;48.
[39] Kaushika ND, Sharma MS, Padmapriya R. Solar thermal analysis of honeycomb roof cover system for energy conservation in an air conditioned building. Energy Build 1992;18:45–9.
[40] Goetzberger A, Dengler J, Rommel M, Gottsche J, Wittwer V. A new transparently insulated, bifacially irradiated solar flat-plate collector. Sol Energy 1992;49:403–11.
[41] Braun PO, Geotzberger A, Schmid J, Stahl W. Transparent insulation of building facades – steps from research to commercial applications. Sol Energy 1992;49:413–27.
[42] Kaushika ND, Padmapriya R. Solar transmittance of honeycomb and parallel slat arrays. Energy Convers Manage 1991;32.
[43] Goetzberger A. Transparent insulation technology for solar energy conversion. 2nd ed. Freiburg: Fraunhofer Institute for Solar Energy Systems; 1991.
[44] Platzer WJ. Solar transmittance of transparent insulation materials. Sol Energy Mater 1987;16.
[45] Kaushika ND, Sharma MS, Sanjay K. Honeycomb roof cover system for passive solar space heating. Energy Convers Manage 1987;27:99–102.
[46] Symons JG. Calculation of the transmittance-absorptance product for flat-plate collectors with convection suppression devices. Sol Energy 1984;33:637–40.
[47] Symons JG. The solar transmittance of some convection suppression devices for solar energy applications: an experimental study. J Sol Energy Eng 1982;104:251–6.
[48] Hollands KGT, Marshall KN, Wedel RK. An approximate equation for predicting the solar transmittance of transparent honeycombs. Sol Energy 1978;21:231–6.
[49] Felland JR, Edwards DK. Solar and infrared radiation properties of parallel-plate honeycomb. J Energy 1978;2:309–17.
[50] Baetens R, Jelle BP, Gustavsen A. Aerogel insulation for building applications: a state-of-the-art review. Energy Build 2011;43:761–9.
[51] Cuce E, Cuce PM, Wood CJ, Riffat SB. Toward aerogel based thermal superinsulation in buildings: a comprehensive review. Renew Sustain Energy Rev 2014;34:273–99.
[52] Gao T, Ihara T, Grynning S, Jelle BP, Lien AG. Perspective of aerogel glazings in energy efficient buildings. Build Environ 2016;95:405–13.
[53] Berardi U. Development of glazing systems with silica aerogel. Energy Proc 2015;78:394–9.
[54] Berardi U. The development of a monolithic aerogel glazed window for an energy retrofitting project. Appl Energy 2015;154:603–15.
[55] Gao T, Jelle BP, Ihara T, Gustavsen A. Insulating glazing units with silica aerogel granules: the impact of particle size. Appl Energy 2014;128:27–34.
[56] Buratti C, Moretti E. Experimental performance evaluation of aerogel glazing systems. Appl Energy 2012;97:430–7.
[57] Wong IL, Eames PC, Perera RS. A review of transparent insulation systems and the evaluation of payback period for building applications. Sol Energy 2007;81:1058–71.
[58] Sun Y, Wu Y, Wilson R, Lu S. Experimental measurement and numerical simulation of the thermal performance of a double glazing system with an interstitial Venetian blind. Build Environ 2016;103:111–22.
[59] Jensen KI, Schultz JM, Kristiansen FH. Development of windows based on highly insulating aerogel glazings. J Non-Cryst Solids 2004;350:351–7.
[60] EASE. Section 3.1 Advanced glazing and transparent insulation. Advanced Glazing. Education of Architecture in Solar Energy and Environment. p. 16–25.
[61] Buratti C, Moretti E. Transparent insulating materials for buildings energy saving: experimental results and performance evaluation. In: Third international conference on applied energy; 2011. p. 1421–32.

[62] Arulanantham M, Kaushika ND. Global radiation transmittance of transparent insulation materials. Sol Energy 1994;53.
[63] Buratti C, Moretti E. Glazing systems with silica aerogel for energy savings in buildings. Appl Energy 2012;98:396–403.
[64] Nordgaard A, Beckman WA. Modelling of flat plate collectors based on monolithic silica aerogel. Sol Energy 1992;49:387–402.
[65] IEA. Solar Heating and Cooling Programme Task 20: Solar Energy in Building Renovation. London: James and James Ltd.; 1997.
[66] Voss K. Solar energy in building renovation– results and experience of international demonstration buildings. Energy Build 2000;32:291–302.
[67] Wallner GM, Lang RW, Schobermayr H, Hegedys H, Hausner R. Development and application demonstration of a novel polymer film based transparent insulation wall heating system. Sol Energy Mater Sol Cells 2004;84:441–57.
[68] Manz H, Egolf PW, Suter P, Goetzberger A. TIM-PCM external wall system for solar space heating and daylighting. Sol Energy 1997;61:369–79.
[69] Twidell JW, Johnstone C, Zuhdy B, Scott A. Strathclyde University's passive solar, low-energy, residences with transparent insulation. Sol Energy 1994;52:85–109.
[70] Bahaj AS, James PAB, Jentsch MF. Potential of emerging glazing technologies for highly glazed buildings in hot arid climates. Energy Build 2008;40:720–31.
[71] Platzer WJ. Advances in Transparent Insulation Technology.
[72] ISO. 8990: Thermal insulation – determination of steady-state thermal transmission properties – calibrated and guarded hot box.; 1996.
[73] ASTM. C1363: Standard Test Method for Thermal Performance of Building Materials and Envelope Assemblies by Means of a Hot Box Apparatus; 2011.
[74] ASTM. C1199: standard test method for measuring the steady-state thermal transmittance of fenestration systems using hot box methods.; 2009.
[75] ISO. 12567-1: thermal performance of windows and doors – determination of thermal transmittance by the hot-box method – part 1: complete windows and doors; 2012.
[76] GOST. 26602.1: windows and doors. Methods of determination of resistance of thermal transmission; 1999.
[77] Yesilata B, Turgut P. A simple dynamic measurement technique for comparing thermal insulation performances of anisotropic building materials. Energy Build 2007;39:1027–34.
[78] Baldinelli G, Bianchi F. Windows thermal resistance: infrared thermography aided comparative analysis among finite volumes simulations and experimental methods. Appl Energy 2014;136:250–8.
[79] Chen F, Wittkopf SK. Summer condition thermal transmittance measurement of fenestration systems using calorimetric hot box. Energy Build 2012;53:47–56.
[80] Asdrubali F, Baldinelli G. Thermal transmittance measurements with the hot box method: calibration, experimental procedures, and uncertainty analyses of three different approaches. Energy Build 2011;43:1618–26.
[81] Fang X. A study of the U-factor of the window with a high-reflectivity venetian blind. Sol Energy 2000;68:207–14.
[82] Fang Y, Eames PC, Norton B, Hyde TJ. Experimental validation of a numerical model for heat transfer in vacuum glazing. Sol Energy 2006;80:564–77.
[83] ISO. 9869-1: Thermal insulation – Building elements – In-situ measurement of thermal resistance and thermal transmittance Part 1: heat flow meter method; 2014.
[84] ASTM. C1046: standard practice for in-situ measurement of heat flux and temperature on building envelope components; 2013.
[85] EN. 673: Glass in building–Determination of thermal transmittance (U value) – calculation method; 2011.
[86] Naylor D, Collins M. Evaluation of an approximate method for predicting the U-value of a window with a between-panes blind. Numer Heat Transf, Part A: Appl 2005;47:233–50.
[87] Collins M, Tasnim S, Wright J. Numerical analysis of convective heat transfer in fenestration with between-the-glass louvered shades. Build Environ 2009;44:2185–92.
[88] Dalal R, Naylor D, Roeleveld D. A CFD study of convection in a double glazed window with an enclosed pleated blind. Energy Build 2009;41:1256–62.
[89] Avedissian T, Naylor D. Free convective heat transfer in an enclosure with an internal louvered blind. Int J Heat Mass Transf 2008;51:283–93.
[90] Giorgi LD, Bertola V, Cafaro E. Thermal convection in double glazed windows with structured gap. Energy Build 2011;43:2034–8.
[91] Almeida F, Naylor D. Experimental study of free convection in a window with a heated between-panes blind. Energy Build 2011;43:2647–55.
[92] Naylor D, Lai BY. Experimental study of natural convection in a window with a between-panes Venetian blind. Exp Heat Transf 2007;20:1–17.
[93] Wright JL, Jin H, Hollands KGT, Naylor D. Flow visualization of natural convection in a tall, air-filled vertical cavity. Int J Heat Mass Transf 2006;49:889–904.
[94] Jonsson A, Roos A, Jonson EK. The effect on transparency and light scattering of dip coated antireflection coatings on window glass and electrochromic foil. Sol Energy Mater Sol Cells 2010;94:992–7.
[95] Long L, Ye H, Zhang H, Gao Y. Performance demonstration and simulation of thermochromic double glazing in building applications. Sol Energy 2015;120:55–64.
[96] Ye H, Long L, Zhang H, Xu B, Gao Y, Kang L, et al. The demonstration and simulation of the application performance of the vanadium dioxide single glazing. Sol Energy Mater Sol Cells 2013;117:168–73.
[97] Goia F, Zinzi M, Carnielo E, Serra V. Spectral and angular solar properties of a PCM-filled double glazing unit. Energy Build 2015;87:302–12.
[98] Gowreesunker BL, Stankovic SB, Tassou SA, Kyriacou PA. Experimental and numerical investigations of the optical and thermal aspects of a PCM-glazed unit. Energy Build 2013;61:239–49.
[99] Liu Xiao, Gao Hao, Sun Yanyi, Yupeng Wu, Martin Benjamin, Chilton John, et al. Thermal and optical analysis of a passive heat recovery and storage system for greenhouse façade/roof. Proc Eng 2016;155:471–8.
[100] Papamichael KM, Klems J, Selkowitz S. Determination and application of bidirectional solar-optical properties of fenesration materials. Technical report LBL-25124. Berkeley: Lawrence Berkeley National Laboratory; 1988.
[101] Klems JH. A new method for predicting the solar heat gain of xomplex fenestration systems. I. Overview and derivation of the matrix layer calculation,. ASHRAE Winter Meeting New Orleans, LA; 1994.
[102] Klems JH, Warner JL. Measurement of bidirectional optical properties of complex shading devices. ASHRAE Trans 1995;101:791–801.
[103] Klems JH, Warner JL, Kelley GO. A comparison between calculated and measured SHGC for complex glazing systems. ASHRAE Trans 1997;102:931–9.
[104] Apian-Bennewitz P, Hardt JVD. Enhancing and calibrating a goniophotometer. Sol Energy Mater Sol Cells 1998;54:309–22.
[105] Breitenbach J, Lart S, Langle I, Rosenfeld JLJ. Optical and thermal performance of glazing with integral venetian blinds. Energy Build 2001;33:433–42.
[106] Andersen M, Rubin M, Powles R, Scartezzini JL. Bi-directional transmission properties of Venetian blinds: experimental assessment compared to ray-tracing calculations. Sol Energy 2005;78:187–98.
[107] Andersen M, Rubin M, Scartezzini J-L. Comparison between ray-tracing simulations and bi-directional transmission measurements on prismatic glazing. Sol Energy 2003;74:157–73.
[108] Reinhart C, Andersen M. Development and validation of a Radiance model for a translucent panel. Energy Build 2006;38:890–904.
[109] Andersen M, de Boer J. Goniophotometry and assessment of bidirectional photometric properties of complex fenestration systems. Energy Build 2006;38:836–48.
[110] Andersen M, de Boer J. Goniophototmetry and assessment of bidirectional photometric properties of complex fenestration systems. In: IEA SHC TASK 31, Daylighting buildings in the 21st century. Stuttgart, Germany; 2005.
[111] Ward G. Measuring and modeling anisotropic reflection. ACM SIGGRAPH Comput Graph 1992;26:265–72.
[112] ISO. 15099: thermal performance of windows, doors and shading devices – detailed calculations; 2003.
[113] Xu X-l, Yang Z. Natural ventilation in the double skin facade with venetian blind. Energy Build 2008;40:1498–504.
[114] Kotey NA, Collins MR, Wright JL, Jiang T. A simplified method for calculating the effective solar optical properties of a Venetian blind layer for building energy simulation. J Sol Energy Eng 2009;131:021002.
[115] Gomes MG, Rodrigues AM, Bogas JA. Numerical and experimental study of the optical properties of venetian blinds. J Build Phys 2012;36:7–34.
[116] Gomes MG, Santos AJ, Rodrigues AM. Solar and visible optical properties of glazing systems with venetian blinds: numerical, experimental and blind control study. Build Environ 2014;71:47–59.
[117] Chaiyapinunt S, Khamporn N. Shortwave thermal performance for a glass window with a curved venetian blind. Sol Energy 2013;91:174–85.
[118] Chaiyapinunt S, Worasinchai S. Development of a mathematical model for a curved slat venetian blind with thickness. Sol Energy 2009;83:1093–113.
[119] Chaiyapinunt Somsak, Khamporn Nopparat. Heat transmission through a glass window with a curved venetian blind installed. Sol Energy 2014;110:71–82.
[120] Somsak Chaiyapinunt, Worasinchai S. Development of a model for calculating the longwave optical properties and surface temperature of a curved venetian blind. Sol – Energy 2009;83:817–31.
[121] Tzempelikos A. The impact of venetian blind geometry and tilt angle on view, direct light transmission and interior illuminance. Sol Energy 2008;82:1172–91.
[122] Boer Jd. Numerical goniophotometer. Stuttgart: User Manual. Fraunhofer Institute of Building Physics; 2004.
[123] Ward G, Shakespeare R. Rendering with radiance: the art and science of lighting visualization. Revised Edition BookSurge, LLC; 2004.
[124] Peng J, Curcija DC, Lu L, Selkowitz SE, Yang H, Mitchell R. Developing a method and simulation model for evaluating the overall energy performance of a ventilated semi-transparent photovoltaic double-skin facade. Prog Photovolt Res Appl 2016;24:781–99.
[125] Peng J, Lu L, Yang H, Ma T. Validation of the Sandia model with indoor and outdoor measurements for semi-transparent amorphous silicon PV modules. Renew Energy 2015;80:316–23.
[126] Huang Y, Niu J-l, Chung T-M. Comprehensive analysis on thermal and daylighting performance of glazing and shading designs on office building envelope in cooling-dominant climates. Appl Energy 2014;134:215–28.
[127] Ihara T, Gustavsen A, Jelle BP. Effect of facade components on energy efficiency in office buildings. Appl Energy 2015;158:422–32.
[128] Bartosz A. Lomanowski JLW. Modeling fenestration with shading devices in buiding energy simulation: a practical approach. In: Eleventh international IBPSA conference. Glasgow, Scotland; 2009.
[129] Anđelković AS, Mujan I, Dakić S. Experimental validation of a EnergyPlus model: application of a multi-storey naturally ventilated double skin façade. Energy Build 2016;118:27–36.
[130] Chaiwiwatworakul P, Chirarattananon S. A double-pane window with enclosed horizontal slats for daylighting in buildings in the tropics. Energy Build 2013;62:27–36.
[131] Firląg S, Yazdanian M, Curcija C, Kohler C, Vidanovic S, Hart R, et al. Control algorithms for dynamic windows for residential buildings. Energy Build 2015;109:157–73.
[132] Hoffmann S, Lee ES, McNeil A, Fernandes L, Vidanovic D, Thanachareonkit A. Balancing daylight, glare, and energy-efficiency goals: an evaluation of exterior coplanar shading systems using complex fenestration modeling tools. Energy Build 2016;112:279–98.

[133] Oh MH, Lee KH, Yoon JH. Automated control strategies of inside slat-type blind considering visual comfort and building energy performance. Energy Build 2012;55:728–37.
[134] Yoon YB, Kim DS, Lee KH. Detailed heat balance analysis of the thermal load variations depending on the blind location and glazing type. Energy Build 2014;75:84–95.
[135] Hoffmann S, Lee ES, Clavero C. Examination of the technical potential of near-infrared switching thermochromic windows for commercial building applications. Sol Energy Mater Sol Cells 2014;123:65–80.
[136] Reinhart C, Fitz A. Findings from a survey on the current use of daylight simulations in building design. Energy Build 2006;38:824–35.
[137] Wong IL, Eames PC, Perera RS. Energy simulations of a transparent-insulated office façade retrofit in London, UK. Smart Sustain Built Environ 2012;1:253–76.